Welcome New GSA Members!

GSA TODAY

THE GEOLOGICAL SOCIETY OF AMERICA®

VOL. 33, NO. 2 | FEBRUARY 2023

New Insights into Feeder Dike Swarms in Scoria Cones and Their Structural Control: A Case Study in the Michoacán-Guanajuato Volcanic Field

New Insights into Feeder Dike Swarms in Scoria Cones and Their Structural Control: A Case Study in the Michoacán-Guanajuato Volcanic Field

Martha Gabriela Gómez-Vasconcelos*, *CONACYT–Instituto de Investigaciones en Ciencias de la Tierra, Universidad Michoacana de San Nicolás de Hidalgo, Morelia, Michoacán, México, gabriela.gomez@umich.mx;* ***Denis-Ramón Avellán,*** *CONACYT–Instituto de Geofísica, Universidad Nacional Autónoma de México, Morelia, Michoacán, México, denisavellan@gmail.com;* ***José Luis Macías, Guillermo Cisneros-Máximo,*** *Instituto de Geofísica, Universidad Nacional Autónoma de México, Morelia, Michoacán, México, jlmv63@gmail.com, gcisneros@igeofisica.unam.mx;* ***Juan Manuel Sánchez -Núñez,*** *Instituto Politécnico Nacional–CIIEMAD, Gustavo A. Madero, Ciudad de México, México, jsancheznu@ipn.mx;* ***Daniel P. Miggins,*** *$^{40}Ar/^{39}Ar$ Geochronology Laboratory, College of Earth, Ocean, and Atmospheric Sciences, Oregon State University, Corvallis, Oregon 97331, USA, daniel.miggins@oregonstate.edu*

ABSTRACT

Understanding the feeder systems in scoria cones is essential because they serve as the conduits that feed the most common eruptions worldwide. Feeder dikes and their emplacement are presumably controlled by the tectonic stress field. However, the mechanism of dike propagation and structural control in monogenetic scoria cones remains poorly understood, as well as the conditions that allow dike swarms in scoria cones and in low magma-flux monogenetic volcanic fields.

This is the first direct study of a magma feeder system in the Michoacán-Guanajuato Volcanic Field in central México. Quarrying in the Cerrito Colorado scoria cone displays six orthogonal feeder dikes—four of them are N-S oriented, parallel to the least compressive stress, intruding preexisting faults, and two are E-W oriented, perpendicular to the least compressive stress, forming their own fracture at the time of the eruption.

Single feeder dikes are common in monogenetic volcanoes, but dike networks (swarms) can develop locally in the vicinity of scoria cones and other vent structures. We suggest that bifurcation of feeder dikes can result from temporary blockages of the conduit and during changes in the magma ascent rate and magma pressure. Feeder dikes at the surface can appear as tabular dikes, cylindrical conduits, or as a combination of both geometries. We suggest that tabular dikes splay-off tangentially, and cylindrical conduits bifurcate radially and axially to the main vent. Our study attests to the complexity and structural control that even small scoria cones can present.

INTRODUCTION

Scoria cones are the most common volcanic form globally, placing countless neighboring populations at risk (Valentine and Gregg, 2008). They form from explosive Strombolian eruptions fed through planar magma-filled conduits, which constitute a feeder dike when magma cools and solidifies (Valentine and Keating, 2007; Tibaldi, 2015). Feeder-dike systems play an essential role in eruptive dynamics (Carracedo-Sánchez et al., 2017); therefore, understanding the role they play is crucial for identifying factors controlling their emplacement and for further forecasting volcanic hazards. However, feeder dikes are poorly understood because they are rarely exposed (Re et al., 2016), and their direct study represents a big challenge for volcanologists. They are usually inferred from seismicity and other geophysical methods (Belachew et al., 2011).

The magma plumbing system in monogenetic scoria cones often consists of a single feeder dike (Németh and Kereszturi, 2015). Nevertheless, some studies suggest it can be composed of an interconnected dike-sill network (Muirhead et al., 2016; Foucher et al., 2018). In addition, the regional and local stress fields frequently control the dike propagation through a newly formed fracture in the upper crust (Connor et al., 2000; Acocella and Neri, 2009), and often, a dike intrusion can use a preexisting fault as a pathway to the surface (Le Corvec et al., 2013). However, the conditions that allow it to intrude a preexisting fault are still discussed (e.g., Valentine and Krogh, 2006), and little is known about the factors that govern a feeder dike bifurcation.

In central México, the Michoacán-Guanajuato Volcanic Field (MGVF) is ideal for studying feeder dikes in monogenetic scoria cones. There are ~900 scoria cones (Hasenaka and Carmichael, 1985), and many of them are exploited as quarries where the feeder-dike system is at times left exposed. However, no feeder dike has been studied in detail. This study presents a direct survey of the Cerrito Colorado scoria cone's feeder-dike system in the MGVF, explored through geological, structural, and drone spatial data. Cerrito Colorado offers unprecedented three-dimensional exposure of its plumbing system, allowing a detailed survey of its geometry and the factors that control the magma emplacement.

VOLCANO-TECTONIC SETTING

The Cerrito Colorado scoria cone sits in the Bajío basin, at the northernmost part of the MGVF within the Trans-Mexican Volcanic Belt's (TMVB) central portion (Fig. 1). The TMVB is a Neogene E-W–oriented 1000-km-long continental volcanic arc related to the Cocos and Rivera plates' subduction along the Middle America trench (Demant, 1978; Pardo and Suárez, 1995). The MGVF is a late Pliocene–Quaternary volcanic field (Hasenaka and Carmichael, 1985) that occurs in an N-S to

GSA Today, v. 33, https://doi.org/10.1130/GSATG539A.1.

*Corresponding author

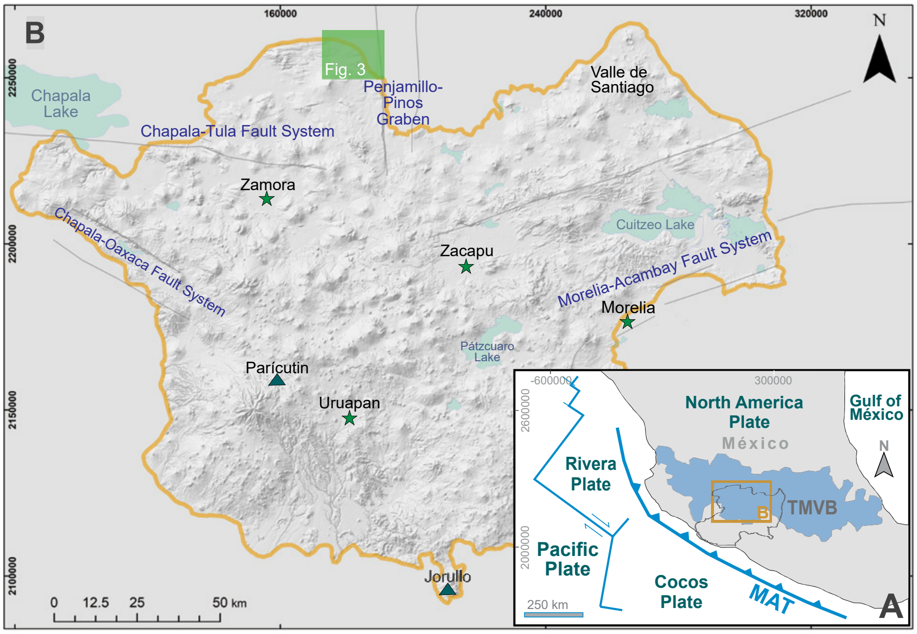

Figure 1. (A) Tectonic setting of the Trans-Mexican Volcanic Belt (TMVB) in central México. (B) Location of the study area (green box; Fig. 3) in the northern Michoacán-Guanajuato Volcanic Field; represented as an orange box in A and an orange polygon in B. MAT—Middle-American Trench.

NNW-oriented extensional tectonic regime (Suter et al., 2001), where volcanoes spatially coincide with three regional active fault systems: N-S, E-W, and NE-SW. N-S–oriented faults belonging to the southern Basin and Range province originated 30 m.y. ago as normal faults and are still active today as dextral strike-slip faults (Aguirre-Díaz and McDowell, 1993). This fault system controlled the formation of the N-S normal faults in the study area and the Penjamillo-Pinos Graben east of the Cerrito Colorado scoria cone (Fig. 1). The E-W–trending faults, known as the Chapala-Tula fault system, originated 19 m.y. ago as sinistral strike-slip faults, and today they are active as normal faults with a sinistral component (Johnson and Harrison, 1989; Garduño-Monroy et al., 2009). E-W–oriented faults control the formation and evolution of lacustrine basins and grabens in central México. The NE-SW faults correspond to a transfer fault system acting as normal to oblique-slip faults. These faults exhibit a significant structural control for the volcanic spatial distribution and geothermal manifestations (Gómez-Vasconcelos et al., 2020; Olvera-García et al., 2020).

METHODS

A microdrone MD-200 aerial vehicle was used to model the volcano and exposed feeder dikes. A photogrammetric flight was performed at the height of 120 m above the volcano (~1890 m above sea level), allowing us to obtain 471 multispectral stereoscopic photographs with a spatial resolution of 30 cm (scale 1:30) in seven photogrammetric flights. Photogrammetric images were processed and georeferenced (coordinate system: WGS 1984 UTM 13N) using the GeoSuite software to construct 3D models and orthoimages. A digital elevation model (DEM) and an orthomosaic were generated in Agisoft Metashape Pro to perform a geomorphological analysis identifying volcanic geoforms, dikes, and faults. The geomorphic characterization of Cerrito Colorado was done with the orthomosaic, 3D model and a Google Earth timelapse for 1985, because, at this moment, the volcano is partially destroyed by quarrying activities.

The volume was calculated with the following equation:

$$V = H\left(BD^2 + BD * CD + CD^2\right)/12, \quad (1)$$

where V is the volume, H is the height, BD is the basal diameter, and CD is the crater diameter.

A rock sample from the main feeder dike was analyzed at the Oregon State University (OSU) Argon Geochronology Lab to determine the age of the Cerrito Colorado volcano. A groundmass separate was irradiated for 30 min in the TRIGA Reactor along with the neutron fluence monitor mineral Fish Canyon Tuff flux monitor with a calibrated age of 28.201 ± 0.023 Ma (1σ) after Kuiper et al. (2008). The $^{40}Ar/^{39}Ar$ age was obtained by incrementally heating the material using a defocused 25-watt CO_2 laser. The resulting gasses were analyzed using an ARGUS-VI multi-collector mass spectrometer. A more detailed analytical method is available from the OSU Argon Lab.

Structural data were obtained in the field by directly measuring tectonic structures (strike, dip, kinematics) and dikes (strike, dip, thickness). Structural lineaments were traced in ArcMap, and the CoGo tool was used to obtain their direction, which was plotted in a rose diagram with Rozeta software. Dihedral angle diagrams were computed using Win_Tensor 5.8.8 with kinematic fault-slip data based on the Angelier stress ratio in the study area.

CERRITO COLORADO SCORIA CONE

The Cerrito Colorado is an NNW-elongated scoria cone with a low topographic profile. It had a basal diameter of 0.6 km, a crater diameter of 0.08 km, a height of 0.04 km, an area of 0.35 km^2, and a volume of 0.0003 km^3. However, nearly 50% has been destroyed by quarrying activities. Pyroclastic deposits associated with this scoria cone consist of non-welded reddish diffuse stratified to massive successions of well to poorly sorted scoria fall deposits. Fall deposits consist of coarse lapilli fragments interstratified with fine lapilli fragments and a low percentage of bread-crust scoria bombs, though ballistic content increases in the western part of the cone (Fig. 2A). Scoria lapilli and bombs show porphyritic textures with plagioclase, olivine, and pyroxene phenocrysts. Scoria is altered to reddish, and fissures are often filled with silica minerals. We dated groundmass from a juvenile fragment using $^{40}Ar/^{39}Ar$ geochronology that yielded a plateau age of 1.68 ± 0.02 Ma. Cerrito Colorado overlies an undifferentiated thick, aphanitic basaltic lava plateau of unknown age.

Feeder Dikes Characterization

The magma plumbing system of Cerrito Colorado is exposed due to quarrying activities. It comprises a network of orthogonal and interconnected conduits presenting two main directions: N-S and E-W. This dike complex fed the Cerrito Colorado eruption, consisting of six sub-vertical to steeply dipping feeder dikes; four are N-S oriented, and two are E-W oriented.

N-S–oriented dikes—Dike 1 is a tabular dike located in the central part of the scoria

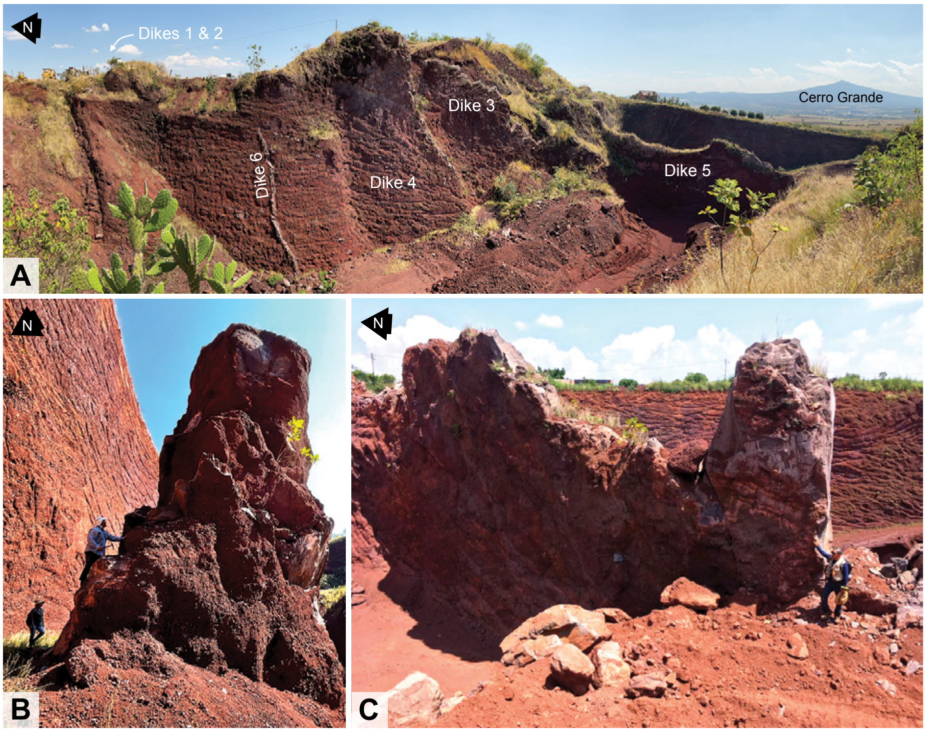

Figure 2. (A) Quarry outcrops showing the orthogonal dike complex in Cerrito Colorado scoria cone and ballistic-rich deposits in the western portion of the volcano. (B) Aspect of dike 2 showing a cylindrical structure. (C) Dike 1: Main N-striking tabular feeding conduit.

cone. It is 180 m long at the surface and 1.1–1.9 m thick. It strikes 006° on average, but in the northern part changes to 023° and dips 82° mainly to the E. This dike shows vertical striae. Dike 2 is 60 m E of dike 1. It is a tabular dike that presents a cylindrical geometry at a shallower depth (>8 m depth) in its northern part. The tabular portion is 130 m long and 0.4–1.1 m thick. The cylindrical portion measures 6 m in diameter at 8-m -depth with 0.3-m -thick annular walls, diminishing to 2.5 m in diameter at the surface (Fig. 2B). It strikes 186° and dips 85° to the W on average, but in its southern part, it dips to the E (supplemental material Fig. S1B[1]). Dike 3 is 50 m W of dike 1. It is a tabular 70-m-long and 1–1.1-m-thick structure. On average, it strikes 001° and dips 83° to the E. Dike 4 is 10 m west of dike 3, showing a left-stepped en échelon geometry. It is a tabular 80-m-long and 0.5–1-m-thick conduit. It strikes 351° and dips 80°E on average (Figs. 2 and 3).

E-W–oriented dikes—Dike 5 is a tabular conduit in the central part of the scoria cone. It crosscuts and is perpendicular to dike 3. It is 120 m long and 1.5 m thick. It strikes 98° and dips 80° to the S on average. Dike 6 lies 70 m north of dike 5. It shows a tabular geometry, and it crosscuts and is perpendicular to dike 4. It is at least 20 m long and 0.4–0.5 m thick. It strikes 069° and dips 83°S on average (Figs. 2 and 4).

All dikes display a single brecciated chilled and dense margin and a vesicular core. Vesicles are spherical toward the periphery, larger and vertically elongated toward the core. All dikes seem to have arrived all the way to the surface, feeding the eruption (see the free-surface effect on dike 2; Fig. S1B [see footnote 1]); except for dike 6, which may have not reached the surface (at least not the exposed segment that is 4 m below the surface) (Figs. 2, S1, and S2 [see footnote 1]). Dike 1 arrives all the way up to the original cone summit, dikes 1 and 4 preserve on their top the original vegetation, and dikes 3–5 apex contour the original slopes of the volcano.

Characterization of Faults

Regional fault traces and lineaments show three main directions: N-S, E-W, and NE-SW. The E-W direction is the most common, followed by the N-S (Fig. 3B), represented by normal to oblique-slip and dextral to oblique-slip, respectively, en échelon faults. Fault kinematics are revealed by geomorphology, structural data, and regional fieldwork (striae, Riedel structures) and endorsed by previous work. The Cerrito Colorado scoria cone lies on top of a 5-km-long N-S–striking dextral-normal steeply dipping fault (355°/84°E) (Fig. 3).

Faults cut Dikes 1 and 5. Dike 1 is cut by E-W- and NE-SW–striking and steeply dipping (76°N and 85°SE, respectively) faults. Dike 5 is cut by N-S–striking and steeply dipping (82°W) faults that displace the scoria cone's deposits by at least 0.2 m (Fig. S1 and Table S1 [see footnote 1]).

DISCUSSION

Structural Control on Magma Emplacement

The regional tectonic stress field usually controls a dike intrusion's orientation. The geometric aspect of the dike is perpendicular to the least compressive stress ($\sigma3$) (Martí et al., 2016), but its emplacement can be influenced by local preexisting faults or fractures (e.g., Connor et al., 2000), which may or may not be perpendicular to $\sigma3$ at the time of the eruption. Local rotation of principal stresses by 90° may be favored when pressurized magma exceeding $\sigma3$ intercepts a discontinuity like a steeply dipping preexisting fault, easing magma ascent at shallow depths because shear strength here is lower than that of the surrounding rock (Valentine and Krogh, 2006; Gudmundsson, 2020).

The MGVF is a low magma-flux field where dikes and normal faults take up active extension. Here, dikes are prone to intercept a preexisting fault, even if it is not oriented with the principal stresses at the time of the eruption. This results in many N-S and E-W–oriented volcanic alignments along this monogenetic field, which parallel the dominant preexisting fault trends (Cebriá et al., 2011; Gómez-Vasconcelos et al., 2020).

In the Cerrito Colorado scoria cone, N-S dikes 1–4 do not strike normal to the least principal stress ($\sigma3$), and E-W dikes 5–6 strike normal to the least principal stress at the time of the eruption. The usage of preexisting structures by ascending magma is favored in this region because the main fault plane is an active steeply dipping transfer fault parallel to $\sigma3$ and perpendicular to $\sigma2$, the magma pressure exceeds $\sigma3$,

[1]Supplemental Material. Figures S1 and S2: Field pictures. Figure S3: Ar/Ar plateau age plots. Table S1: Characterization of the dike swarm. Go to https://doi.org/10.1130/GSAT.S.20379540 to access the supplemental material; contact editing@geosociety.org with any questions.

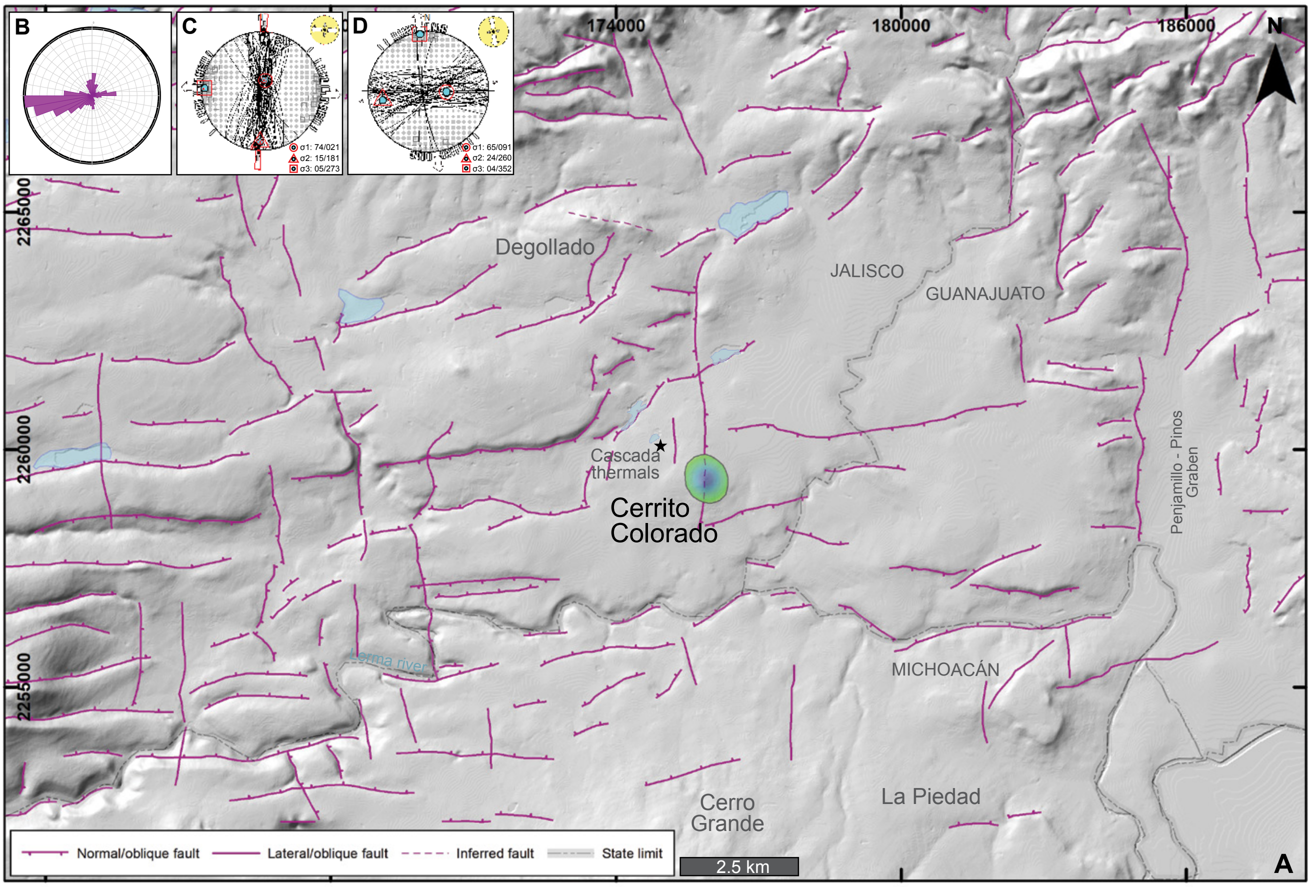

Figure 3. (A) Location of the Cerrito Colorado scoria cone and surrounding fault traces. (B) Rose diagram for the regional and local faults (lower hemisphere projection). (C) Dihedral angle diagram of the Oligocene-Miocene stress field agrees with N-S normal faults and tension fractures. (D) Dihedral angle diagram for the Miocene-present stress field agrees with E-W normal faults and tension fractures. Data computed using Win_Tensor 5.8.8 with kinematic fault slip data in the study area (see structural data in Table S1 [see text footnote 1]).

and the horizontal stress differential between σ3 and σ2 must have been very low at the time of the intrusion (e.g., Yale, 2003; Heidbach et al., 2007). We infer a low horizontal stress ratio because magma overpressure will increase σ3 and thus make it similar to σ2. We also infer this low-stress ratio because both E-W and N-S faults are active under the same regional stress regime; N-S faults act as anti-Riedel structures in a transtensional setting. N-S faults are dextral faults with a normal component and used to act as normal faults in the late Miocene-Oligocene, so are more prone to dilate, allowing a magma pathway to the surface. The fact that dikes are intruding through preexisting N-S faults also evidences that σ3 and σ2 are interchanged. Therefore, the regional tectonic stress field and preexisting tectonic structures conditioned the orientation (spatial distribution) of the Cerrito Colorado feeder-dike system. Further, the ascent of geothermal fluids was also fault-controlled, evidenced by abundant quartz minerals and proximity to the Cascada thermal pools (Fig. 3).

Eruption Evolution and Eruptive Dynamics

The Strombolian-style eruption of Cerrito Colorado had the following dike order: 1, 2/3, 4, 5, 6. We suggest this dike order because of their heights, widths, and cross-cutting relations; dikes 5 and 6 cut dikes 3 and 4, respectively (Figs. 3–5). Magma overpressure diminishes toward the end of the eruption; therefore, we infer larger and wider dikes will come first. The eruption begun with feeder dike 1 (largest and widest dike) arriving at the surface using a preexisting N-S steeply dipping (84°) dextral fault, not coinciding with the stress field at the time of the eruption. We suggest the magma intrusion intercepted the preexisting fault in the shallow crust as it encountered this subvertical E-dipping shear zone. Vertical striae in some parts of feeder dike 1 could denote shearing from vertical magma flow. The emplacement of magma could have also relaxed the friction across the host fault plane, triggering a co-intrusive fault slip if the preexisting fault was near failure (e.g., Gaffney et al., 2007). Eventually, the vent from dike 1 became closed (local implosion) or buried by scoria fragments, revealed by a further propagation of dike 1 to the north and a slight orientation change from N-S to NE-SW, possibly related to its emplacement through weakly consolidated scoria deposits. This orientation change in dike 1 could indicate limited degassing and gas accumulation beneath the surface, causing an overpressure rise (e.g., Valentine and Krogh, 2006). Therefore, new vents had to be formed, allowing the release of pressure through N-S preexisting fractures parallel to the main fault plane (dikes 2, 3, and 4) and through a tangential self-propagating tabular dike coinciding with the stress field at the time of the eruption (parallel to the greatest principal stress; dikes 5 and 6). Synchronously with the first

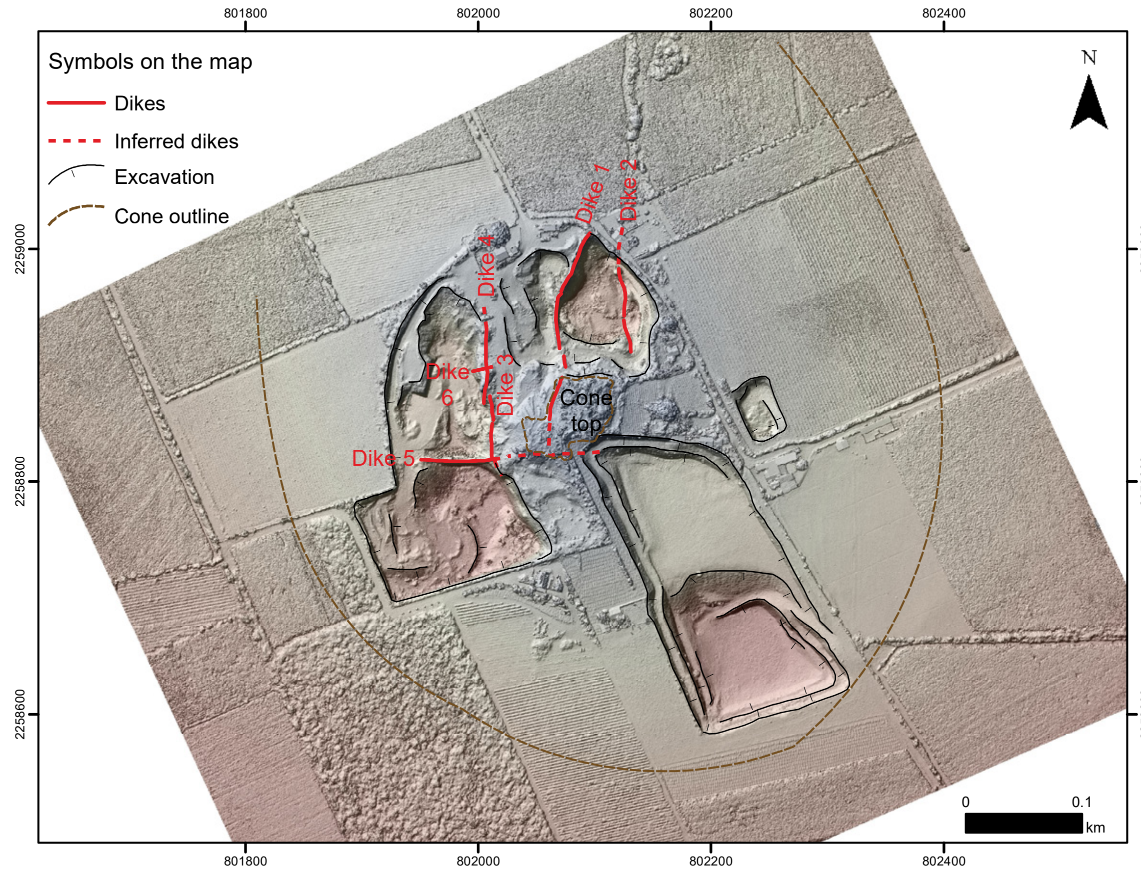

Figure 4. Shaded-relief model of the Cerrito Colorado scoria cone generated with the aerial vehicle. The model allows identifying the quarrying excavation, the exposed dike-feeding system and its cross-cutting relations.

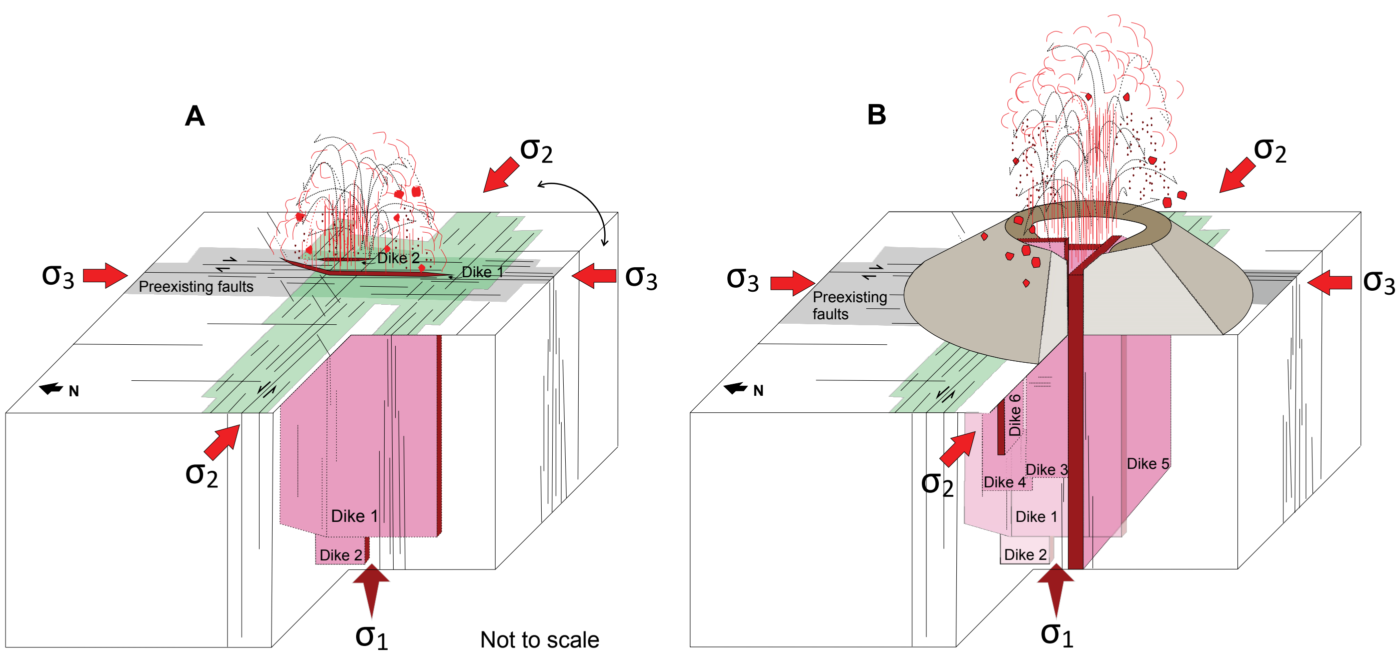

Figure 5. Magma emplacement model for a complex feeder-dike system in monogenetic scoria cones. (A) Magma encounters a stress barrier and intrudes a steeply dipping dextral-normal N-S preexisting fault parallel to the least principal stress (σ3). (B) Magma bifurcates into 5–6 E-W feeder dikes (orthogonal to 1–4 feeder dikes) through self-propagating fractures coinciding with the stress field at the time of the eruption (normal to the least principal stress).

dike intrusion, magma diverged into a secondary vent: either dikes 2 or 3, assuming dike widths tend to diminish during the eruption (Fig. 5). Dike 2 could have broken out of the main fault plane to propagate vertically at shallow depth (e.g., Connor et al., 2000) all the way to the surface, evidenced by dike 2 chilled margins (Fig. S1 [see footnote 1]). Magma plumbing bifurcation is encouraged with a magma ascent rate increase that creates magma overpressure (e.g., Geshi, 2005). The rise in magma's ascent velocity is supported by its transition into a cylindrical mix-flow conduit in its northern part at a shallower depth (<8 m depth; slug flow: continuous gas phase flowing radially and axially; e.g., Suckale et al., 2010; Cashman and Sparks, 2013) denoting a gas-dominated flow that allowed a larger and more stable magma flux (e.g., Costa et al., 2009). The slug flow in the cylindrical conduit could have conditioned a change in the eruptive style (e.g., violent Strombolian activity) where pyroclastic fall deposits become finer-grained and stratified. However, this would need a more detailed granulometric analysis to verify the change in eruptive style. Dikes 3 and 4's new vent opening allowed repressurization of the system with a relatively cool (non-spatter) ballistic-rich eruption and ash-lapilli scoria fragments, typical of a vent-opening stage (e.g., Thivet et al., 2020). Since dikes 1, 2, 3, and 4 dip E, bomb-rich deposits mainly lie on the western part of the scoria cone (Fig. 2A). Subsequently, an E-W dike formed (dike 5) through a new tangential self-propagating vent perpendicular to $\sigma3$. Dikes 4 and 6 show thinner and irregular widths because they intruded through unconsolidated scoria fragments. The last dike (thinner dike: dike 6) did not reach the surface to feed the eruption, probably because at this stage of the eruption, the magma overpressure was reduced and did not exceed $\sigma3$. It is possible that dike 1 continued actively throughout the eruption because it lies higher than the other dikes and arrives all the way up to the original cone summit.

CONCLUSIONS

Studying the interior of a scoria cone and its magma plumbing system is a great challenge for volcanologists. Nonetheless, quarrying activities in the MGVF help with the direct study of these structures.

This is the first direct and detailed study of a magma feeding system in a monogenetic scoria cone in México. Our study supports many analog models and theoretical studies, providing new and direct evidence for magma emplacement in low-magma–flux regions. We propose that at least two ingredients are needed for an orthogonal dike swarm growth in monogenetic scoria cones: (1) relatively similar (isotropic) horizontal principal stresses ($\sigma3$ and $\sigma2$) in order to be interchanged; and (2) changes in local magmatic pressure (magma overpressure, poor degassing, or high flow rates at the surface). Moreover, we suggest that tabular dikes bifurcate tangentially (at times en échelon), and cylindrical vents bifurcate radially (annular geometry) and axially to the main conduit derived from local magma overpressure and centrifugal force.

In transtensional, low-magma–flux regions (e.g., MGVF), dike intrusions are tectonically controlled by regional and local stress fields and can easily develop orthogonal dike systems. Dike intrusions at shallow depths can intercept a preexisting fault that may or may not be perpendicular to $\sigma3$ at the time of the eruption, especially when magma is overpressured and when preexisting faults are steeply dipping (>75°) and parallel or perpendicular to $\sigma3$.

Our study attests that Strombolian eruptions are very unstable. Even slight local changes in magma pressure or stress field (caused by local stress barriers like preexisting structures) can alter their feeding system, inducing changes in the eruption dynamics with important implications on their volcanic hazard. The feeder system to the Cerrito Colorado eruption was controlled by N-S preexisting structures, the regional and local tectonic stress field, and magma pressure changes.

ACKNOWLEDGMENTS

We are grateful to Jorge Lara, Nestor Fitz, and Karla Cruz for their valuable support during fieldwork. We also thank Jim Schmitt (*GSA Today* science editor), James Muirhead and Abdelsalam Elshaafi (reviewers), and Pilar Villamor for their valuable feedback, which improved our manuscript quality. This study was funded by project A1-S-23296 (CONACYT) to Dr. Avellán.

REFERENCES CITED

Acocella, V., and Neri, M., 2009, Dike propagation in volcanic edifices: Overview and possible developments: Tectonophysics, v. 471, no. 1–2, p. 67–77, https://doi.org/10.1016/j.tecto.2008.10.002.

Aguirre-Díaz, G.J., and McDowell, F.W., 1993, Nature and timing of faulting and synextensional magmatism in the southern Basin and Range, central-eastern Durango, Mexico: Geological Society of America Bulletin, v. 105, no. 11, p. 1435–1444, https://doi.org/10.1130/0016-7606(1993)105<1435:NATOFA>2.3.CO;2.

Belachew, M., Ebinger, C., Coté, D., Keir, D., Rowland, J.V., Hammond, J.O., and Ayele, A., 2011, Comparison of dike intrusions in an incipient seafloor-spreading segment in Afar, Ethiopia: Seismicity perspectives: Journal of Geophysical Research. Solid Earth, v. 116, no. B6, https://doi.org/10.1029/2010JB007908.

Carracedo-Sánchez, M., Sarrionandia, F., Abalos, B., Errandonea-Martin, J., and Ibarguchi, J.G., 2017, Intra-cone plumbing system and eruptive dynamics of small-volume basaltic volcanoes: A case study in the Calatrava Volcanic Field: Journal of Volcanology and Geothermal Research, v. 348, p. 82–95, https://doi.org/10.1016/j.jvolgeores.2017.10.014.

Cashman, K.V., and Sparks, R.S.J., 2013, How volcanoes work: A 25-year perspective: Geological Society of America Bulletin, v. 125, no. 5–6, p. 664–690, https://doi.org/10.1130/B30720.1.

Cebriá, J.M., Martín-Escorza, C., López-Ruiz, J., Morán-Zenteno, D.J., and Martiny, B.M., 2011, Numerical recognition of alignments in monogenetic volcanic areas: Examples from the Michoacán-Guanajuato Volcanic Field in Mexico and Calatrava in Spain: Journal of Volcanology and Geothermal Research, v. 201, no. 1–4, p. 73–82, https://doi.org/10.1016/j.jvolgeores.2010.07.016.

Connor, C.B., Stamatakos, J.A., Ferrill, D.A., Hill, B.E., Ofoegbu, G.I., Conway, F.M., Sagar, B., and Trapp, J., 2000, Geologic factors controlling patterns of small□volume basaltic volcanism: Application to a volcanic hazards assessment at Yucca Mountain, Nevada: Journal of Geophysical Research. Solid Earth, v. 105, no. B1, p. 417–432, https://doi.org/10.1029/1999JB900353.

Costa, A., Sparks, R.S.J., Macedonio, G., and Melnik, O., 2009, Effects of wall-rock elasticity on magma flow in dykes during explosive eruptions: Earth and Planetary Science Letters, v. 288, no. 3–4, p. 455–462, https://doi.org/10.1016/j.epsl.2009.10.006.

Demant, A., 1978, Características del Eje Neovolcánico Transmexicano y sus problemas de interpretación: Revista Mexicana de Ciencias Geológicas, v. 2, no. 2, p. 172–187.

Foucher, M.S., Petronis, M.S., Lindline, J., and van Wyk de Vries, B., 2018, Investigating the magmatic plumbing system of a monogenetic scoria cone: A field and laboratory study of the Cienega scoria cone, Cerros del Rio Volcanic Field, New Mexico: Geochemistry, Geophysics, Geosystems, v. 19, no. 7, p. 1963–1978, https://doi.org/10.1029/2017GC007222.

Gaffney, E.S., Damjanac, B., and Valentine, G.A., 2007, Localization of volcanic activity: 2. Effects of preexisting structure: Earth and Planetary Science Letters, v. 263, no. 3–4, p. 323–338, https://doi.org/10.1016/j.epsl.2007.09.002.

Garduño-Monroy, V.H., Pérez-Lopez, R., Israde-Alcantara, I., Rodríguez-Pascua, M.A., Szynkaruk, E., Hernández-Madrigal, V.M., García-Zepeda, M.L., Corona-Chávez, P., Ostroumov, M., Medina-Vega, V.H., and García-Estrada, G., 2009, Paleoseismology of the southwestern Morelia-Acambay fault system, central Mexico: Geofísica Internacional, v. 48, no. 3, p. 319–335, https://doi.org/10.22201/igeof.00167169p.2009.48.3.29.

Geshi, N., 2005, Structural development of dike swarms controlled by the change of magma supply rate: The cone sheets and parallel dike swarms of the Miocene Otoge igneous complex, Central Japan: Journal of Volcanology and Geothermal Research, v. 141, no. 3–4, p. 267–281, https://doi.org/10.1016/j.jvolgeores.2004.11.002.

Gómez-Vasconcelos, M.G., Macías, J.L., Avellán, D.R., Sosa-Ceballos, G., Garduño-Monroy, V.H., Cisneros-Máximo, G., Layer, P.W., Benowitz, J., López-Loera, H., López, F.M., and Perton, M., 2020, The control of preexisting faults on the distribution, morphology, and volume of monogenetic volcanism in the Michoacán-Guanajuato Volcanic Field: Geological Society of America Bulletin, v. 132, no. 11–12, p. 2455–2474, https://doi.org/10.1130/B35397.1.

Gudmundsson, A., 2020, Volcanotectonics: Understanding the structure, deformation and dynamics of volcanoes: Cambridge, UK, Cambridge University Press, 598 p., https://doi.org/10.1017/9781139176217.

Hasenaka, T., and Carmichael, I.S., 1985, The cinder cones of Michoacán–Guanajuato, central Mexico: Their age, volume and distribution, and magma discharge rate: Journal of Volcanology and Geothermal Research, v. 25, no. 1–2, p. 105–124, https://doi.org/10.1016/0377-0273(85)90007-1.

Heidbach, O., Reinecker, J., Tingay, M., Müller, B., Sperner, B., Fuchs, K., and Wenzel, F., 2007, Plate boundary forces are not enough: Second- and third-order stress patterns highlighted in the World Stress Map database: Tectonics, v. 26, no. 6, https://doi.org/10.1029/2007TC002133.

Johnson, C.A., and Harrison, C.G.A., 1989, Tectonics and volcanism in central Mexico: A Landsat Thematic Mapper perspective: Remote Sensing of Environment, v. 28, p. 273–286, https://doi.org/10.1016/0034-4257(89)90119-3.

Kuiper, K.F., Deino, A., Hilgen, F.J., Krijgsman, W., Renne, P.R., and Wijbrans, A.J., 2008, Synchronizing rock clocks of Earth history: Science, v. 320, no. 5875, p. 500–504, https://doi.org/10.1126/science.1154339.

Le Corvec, N., Menand, T., and Lindsay, J., 2013, Interaction of ascending magma with preexisting crustal fractures in monogenetic basaltic volcanism: An experimental approach: Journal of Geophysical Research. Solid Earth, v. 118, no. 3, p. 968–984, https://doi.org/10.1002/jgrb.50142.

Martí, J., López, C., Bartolini, S., Becerril, L., and Geyer, A., 2016, Stress controls of monogenetic volcanism: A review: Frontiers of Earth Science, v. 4, p. 106, https://doi.org/10.3389/feart.2016.00106.

Muirhead, J.D., Van Eaton, A.R., Re, G., White, J.D., and Ort, M.H., 2016, Monogenetic volcanoes fed by interconnected dikes and sills in the Hopi Buttes volcanic field, Navajo Nation, USA: Bulletin of Volcanology, v. 78, no. 2, p. 1–16, https://doi.org/10.1007/s00445-016-1005-8.

Németh, K., and Kereszturi, G., 2015, Monogenetic volcanism: Personal views and discussion: International Journal of Earth Sciences, v. 104, no. 8, p. 2131–2146, https://doi.org/10.1007/s00531-015-1243-6.

Olvera-García, E., Garduño-Monroy, V.H., Liotta, D., Brogi, A., Bermejo-Santoyo, G., and Guevara-Alday, J.A., 2020, Neogene-Quaternary normal and transfer faults controlling deep-seated geothermal systems: The case of San Agustin del Maiz (central Trans-Mexican Volcanic Belt, Mexico): Geothermics, v. 86, 101791, https://doi.org/10.1016/j.geothermics.2019.101791.

Pardo, M., and Suárez, G., 1995, Shape of the subducted Rivera and Cocos plates in southern Mexico: Seismic and tectonic implications: Journal of Geophysical Research. Solid Earth, v. 100, no. B7, p. 12,357–12,373, https://doi.org/10.1029/95JB00919.

Re, G., White, J.D., Muirhead, J.D., and Ort, M.H., 2016, Subterranean fragmentation of magma during conduit initiation and evolution in the shallow plumbing system of the small-volume Jagged Rocks volcanoes (Hopi Buttes Volcanic Field, Arizona, USA): Bulletin of Volcanology, v. 78, no. 8, p. 1–20, https://doi.org/10.1007/s00445-016-1050-3.

Suckale, J., Hager, B.H., Elkins-Tanton, L.T., and Nave, J.C., 2010, It takes three to tango: 2. Bubble dynamics in basaltic volcanoes and ramifications for modeling normal Strombolian activity: Journal of Geophysical Research. Solid Earth, v. 115, no. B7, https://doi.org/10.1029/2009JB006917.

Suter, M., Martínez, M.L., Legorreta, O.Q., and Martínez, M.C., 2001, Quaternary intra-arc extension in the central Trans-Mexican volcanic belt: Geological Society of America Bulletin, v. 113, no. 6, p. 693–703, https://doi.org/10.1130/0016-7606(2001)113<0693:QIAEIT>2.0.CO;2.

Thivet, S., Gurioli, L., Di Muro, A., Derrien, A., Ferrazzini, V., Gouhier, M., Coppola, D., Galle, B., and Arellano, S., 2020, Evidences of plug pressurization enhancing magma fragmentation during the September 2016 basaltic eruption at Piton de la Fournaise (La Réunion Island, France): Geochemistry, Geophysics, Geosystems, v. 21, no. 2, e2019GC008611, https://doi.org/10.1029/2019GC008611

Tibaldi, A., 2015, Structure of volcano plumbing systems: A review of multi-parametric effects: Journal of Volcanology and Geothermal Research, v. 298, p. 85–135, https://doi.org/10.1016/j.jvolgeores.2015.03.023.

Valentine, G.A., and Gregg, T.K.P., 2008, Continental basaltic volcanoes—Processes and problems: Journal of Volcanology and Geothermal Research, v. 177, no. 4, p. 857–873, https://doi.org/10.1016/j.jvolgeores.2008.01.050.

Valentine, G.A., and Keating, G.N., 2007, Eruptive styles and inferences about plumbing systems at Hidden Cone and Little Black Peak scoria cone volcanoes (Nevada, USA): Bulletin of Volcanology, v. 70, no. 1, p. 105–113, https://doi.org/10.1007/s00445-007-0123-8.

Valentine, G.A., and Krogh, K.E., 2006, Emplacement of shallow dikes and sills beneath a small basaltic volcanic center—The role of preexisting structure (Paiute Ridge, southern Nevada, USA): Earth and Planetary Science Letters, v. 246, no. 3–4, p. 217–230, https://doi.org/10.1016/j.epsl.2006.04.031.

Yale, D.P., 2003, Fault and stress magnitude controls on variations in the orientation of in situ stress, *in* Ameen, M., ed., Fracture and In-Situ Stress Characterization of Hydrocarbon Reservoirs: Geological Society of London Special Publication 209, p. 55–64, https://doi.org/10.1144/GSL.SP.2003.209.01.06.

Manuscript received 17 Mar. 2022
Revision received 30 June 2022
Manuscript accepted 18 July 2022